

Nonlinear magnetic susceptibility and aging phenomena in reentrant ferromagnet: $\text{Cu}_{0.2}\text{Co}_{0.8}\text{Cl}_2\text{-FeCl}_3$ graphite bi-intercalation compound

Masatsugu Suzuki and Itsuko S. Suzuki†

Department of Physics, State University of New York at Binghamton, Binghamton, New York 13902-6016
(Dated: April 14, 2024)

Linear and nonlinear dynamic properties of a reentrant ferromagnet $\text{Cu}_{0.2}\text{Co}_{0.8}\text{Cl}_2\text{-FeCl}_3$ graphite bi-intercalation compound are studied using AC and DC magnetic susceptibility. This compound undergoes successive phase transitions at the transition temperatures T_h ($= 16$ K), T_c ($= 9.7$ K), and T_{RSG} ($= 3.5$ K). The static and dynamic behaviors of the reentrant spin glass phase below T_{RSG} are characterized by those of normal spin glass phase with critical exponent $\nu = 0.57 \pm 0.10$, a dynamic critical exponent $x = 8.5 \pm 1.8$, and an exponent $p = 1.55 \pm 0.13$ for the de Almeida-Thouless line. A prominent nonlinear susceptibility is observed between T_{RSG} and T_c and around T_h , suggesting a chaotic nature of the ferromagnetic phase ($T_{\text{RSG}} < T < T_c$) and the helical spin ordered phase ($T_c < T < T_h$). The aging phenomena are observed both in the RSG and FM phases, with the same qualitative features as in normal spin glasses. The aging of zero-field cooled magnetization indicates a drastic change of relaxation mechanism below and above T_{RSG} . The time dependence of the absorption χ'' is described by a power law form ($\propto t^{-b^0}$) in the ferromagnetic phase, where $b^0 = 0.074 \pm 0.016$ at $f = 0.05$ Hz and $T = 7$ K. No $\log t$ -scaling law for χ'' ($\propto (\log t)^{b^0}$) is observed.

PACS numbers: 75.40.Gb, 75.50.Lk, 75.30.Kz, 75.70.Cn

I. INTRODUCTION

The nature of a reentrant spin glass (RSG) phase and a ferromagnetic (FM) phase in reentrant ferromagnets has been a topic of much controversy.^{1,2,3,4,5,6,7,8,9,10,11,12,13,14,15} Spin frustration effects occur as a result of a competition between ferromagnetic interactions as a majority and antiferromagnetic interactions as a minority. As the temperature is lowered, the reentrant ferromagnet exhibits first a transition from a paramagnetic (PM) phase to a FM phase with decreasing temperature and then a second transition from the FM phase to a RSG phase. Such a reentry behavior of the reentrant ferromagnets has been extensively studied experimentally in the last two decades.^{1,2,3,4,5,6,7,8,9,10,11,12,13,14,15} There are four types of reentrant ferromagnets: (i) metallic spin glasses such as $\text{Fe}_{0.7}\text{Al}_{0.3}$,^{1,2} $(\text{Fe}_{0.20}\text{Ni}_{0.80})_{75}\text{P}_{16}\text{B}_6\text{Al}_3$,^{3,4,5} $(\text{Fe}_{1-x}\text{Mn}_x)_{75}\text{P}_{16}\text{B}_6\text{Al}_3$ ($0.2 < x < 0.32$),⁶ and $\text{Ni}_{77}\text{Mn}_{22}$ ^{7,8} having Ruderman-Kittel-Kasuya-Yosida (RKKY)-type interactions between distant spins, (ii) insulating spin glasses such as $\text{CdCr}_{2-x}\text{In}_{2(x)}\text{S}_4$ ($0.90 < x < 1$),^{9,10,11,12} (iii) dilute magnetic semiconductors such as $\text{Eu}_x\text{Sr}_{1-x}\text{S}$ ($0.52 < x < 0.60$),^{13,14} and (iv) colossal magnetoresistance materials such as $\text{Y}_{0.7}\text{Ca}_{0.3}\text{MnO}_3$.¹⁵ In the case of (ii) and (iii), ferromagnetic nearest neighbor interactions compete with antiferromagnetic next nearest neighbor interactions.

The nature of the RSG and FM phases in reentrant ferromagnets is basically understood in terms of a mean-field picture. The phase diagram (T vs J_0/J) of the Sherrington-Kirkpatrick (SK) model with Ising spins,¹⁶ consists of the PM phase, FM phase, and the spin glass (SG) phase, where an infinite-ranged Gaussian distribution of exchange interactions with variance J and mean

J_0 is assumed.¹⁷ For $J_0/J = 1$, as T is lowered, the system undergoes a transition from the PM phase to the SG phase. For $J_0/J > 1$, as T is lowered, the system undergoes a PM-FM transition followed by a FM-SG transition. This SG phase for $J_0/J > 1$ is called a RSG phase. However, the nature of the RSG phase is essentially the same as that of the normal SG phase for $J_0/J = 1$. When the Parisi's solution for the SK model^{18,19} is discovered, the vertical phase boundary at $J_0/J = 1$ is added to the SK phase diagram. For $J_0/J > 1$, consequently the whole RSG phase and a part of the FM phase in the SK model are newly replaced by a RSG phase with replica symmetry breaking (RSB). This RSG phase is very different from the normal SG phase for $J_0/J = 1$. It is a mixed phase of the SG phase and the FM phase.

In the mean-field picture, a true reentrance from the FM phase to the normal SG phase is not predicted. There is a normal FM long-range order in the FM phase. This picture, which assumes infinite-range interactions, is not always appropriate for real reentrant magnets where the short-range interactions are large and random in sign and the spin symmetry is rather Heisenberg-like than Ising-like. Neutron scattering studies on $(\text{Fe}_{1-x}\text{Mn}_x)_{75}\text{P}_{16}\text{B}_6\text{Al}_3$ ⁶ have questioned the existence of a true long-range order even in the FM phase. Aeppli et al.⁶ have proposed a phenomenological random-field picture to explain their result. In this picture, the system in the FM phase consists of regions which would order ferromagnetically and other regions forming PM clusters. The frustrated spins in the PM clusters can generate random molecular fields, which act on the unfrustrated spins in the infinite FM network. In the FM phase well above T_{RSG} , the fluctuations of the spins in the PM clusters are so rapid that the FM network is less influenced by them and their effect is only to reduce the

net FM moment. On decreasing the temperature toward T_{RSG} , the thermal fluctuations of the spins in the PM clusters become slower. The coupling between the PM clusters and the FM network becomes important and the molecular field from the slow PM spins acts as a random magnetic field. This causes breakups of the FM network into finite-sized clusters. Below T_{RSG} , the ferromagnetism completely disappears, leading to a SG phase. This picture is very different from the mean-field picture. The RSG phase is not a mixed phase but a normal SG phase.

Jonason et al.^{4,5} have shown from a dynamic scaling analysis of low-field dynamic susceptibility of $(Fe_{0.20}Ni_{0.80})_{75}P_{16}B_6A_3$ that there is a spin-glass relaxation time which diverges at a finite temperature with a dynamic critical exponent similar to that observed for an ordinary PM-SG transition. This suggests that the RSG phase is a normal SG phase. The FM phase just above T_{RSG} shows a dynamic behavior characterized by an aging effect and chaotic nature similar to that of SG phase. Dupuis et al.¹² have shown that the aging behavior of the low frequency AC susceptibility is observed both in the FM phase and RSG phase of $CdCr_{2-x}In_{2(1-x)}S_4$ with $x = 0.90, 0.95$, and 1.00 , with the same qualitative features as in normal spin glasses. It seems that these results are explained in terms of the random-field picture.

In this paper we report our experimental study on the magnetic properties of the RSG phase and the FM phase of a reentrant ferromagnet $Cu_{0.2}Co_{0.8}C_2$ -FeCl₃ graphite bi-intercalation compound (GBIC). This compound undergoes three phase transitions at T_h ($= 16$ K), T_c ($= 9.7$ K), and T_{RSG} ($= 3.5$ K). There are the helical spin ordered phase between T_h and T_c , the FM phase between T_c and T_{RSG} , and the RSG phase below T_{RSG} .^{20,21,22,23} The static and dynamic natures of the FM and RSG phases are examined from the linear and nonlinear AC magnetic susceptibility, the magnetizations in the zero-field cooled (ZFC), field-cooled (FC), isothermal remnant (IR), and thermomagnetic remnant (TR) states. The time dependence of the AC susceptibility and the ZFC magnetization, showing the aging phenomena, is also studied.

$Cu_{0.2}Co_{0.8}C_2$ -FeCl₃ GBIC has a unique layered structure where the $Cu_{0.2}Co_{0.8}C_2$ intercalate layer ($= I_1$) and FeCl₃ intercalate layers ($= I_2$) alternate with a single graphite layer (G), forming a stacking sequence (-G-I₁-G-I₂-G-I₁-G-I₂-G-) along the c axis. In the $Cu_{0.2}Co_{0.8}C_2$ intercalate layer two kinds of magnetic ions (Cu^{2+} and Co^{2+}) are randomly distributed on the triangular lattice. The spin order in the $Cu_{0.2}Co_{0.8}C_2$ layers is coupled with that in the FeCl₃ intercalate layer ($= I_2$) through an interplanar exchange interaction, leading to the spin frustration effect.

II. EXPERIMENTAL PROCEDURE

A sample of stage-2 $Cu_{0.2}Co_{0.8}C_2$ graphite intercalation compound (GIC) as a starting material was pre-

pared from single crystalline graphite (SCKG) by vapor reaction of anhydrous $Cu_{0.2}Co_{0.8}C_2$ in a chlorine atmosphere with a gas pressure of 740 Torr.^{20,21,22,23} The reaction was continued at 500 °C for three weeks. The sample of $Cu_{0.2}Co_{0.8}C_2$ -FeCl₃ GBIC was prepared by a sequential intercalation method: the intercalant FeCl₃ was intercalated into empty graphite galleries of stage-2 $Cu_{0.2}Co_{0.8}C_2$ GIC. A mixture of well-defined stage-2 $Cu_{0.2}Co_{0.8}C_2$ GIC based on SCKG and single-crystal FeCl₃ was sealed in vacuum inside Pyrex glass tubing, and was kept at 330 °C for two weeks. The stoichiometry of the sample is represented by $C_m(Cu_{0.2}Co_{0.8}C_2)_{1-x}(FeCl_3)_x$. The concentration of C and Fe (m and x) was determined from weight uptake measurement and electron microprobe measurement [using a scanning electron microscope (Model Hitachi S-450)]: $m = 7.54 \pm 0.05$ and $x = 0.56 \pm 0.02$. The (00L) x-ray diffraction measurements of stage-2 $Cu_{0.2}Co_{0.8}C_2$ GIC and $Cu_{0.2}Co_{0.8}C_2$ -FeCl₃ GBIC were made at 300 K by using a Huber double circle diffractometer with a MoK α x-ray radiation source (1.5 kW). The c-axis repeat distance of stage-2 $Cu_{0.2}Co_{0.8}C_2$ GIC and $Cu_{0.2}Co_{0.8}C_2$ -FeCl₃ GBIC was determined as 12.81 \pm 0.04 and 18.79 \pm 0.05 Å, respectively.

The DC magnetization and AC susceptibility were measured using a SQUID magnetometer (Quantum Design, MPMSXL-5) with an ultra low-field capability option. First a remnant magnetic field was reduced to zero field (exactly less than 3 mOe) at 298 K for both DC magnetization and AC susceptibility measurements. Then the sample was cooled from 298 to 1.9 K in a zero field. (i) Measurements of the zero field cooled susceptibility (ZFC) and the field cooled susceptibility (FC). After an external magnetic field H ($0 < H \leq 5$ kOe) was applied along the c plane (basal plane of graphene layer) at 1.9 K, ZFC was measured with increasing temperature (T) from 1.9 to 20 K. After annealing of sample for 10 minutes at 100 K in the presence of H , FC was measured with decreasing T from 20 to 1.9 K. (ii) AC susceptibility measurement. The frequency (f), magnetic field, and temperature dependence of the dispersion (χ'') and absorption (χ'') was measured between 1.9 to 20 K, where the frequency of the AC field is $f = 0.01 - 1000$ Hz and the amplitude h is typically $h = 1 \text{ mOe} - 4.2 \text{ Oe}$.

III. RESULT

A. Nonlinear AC susceptibility: χ'' and χ''

We have measured the dispersion χ'' and absorption χ'' at fixed T as a function of h , where $1 \text{ mOe} < h < 4.2 \text{ Oe}$ and $f = 1 \text{ Hz}$. Both χ'' and χ'' are strongly dependent on h , suggesting the existence of nonlinear magnetic susceptibility. We determine the T dependence of nonlinear AC magnetic susceptibilities (χ'' , χ'' , χ'' , χ'') from the least squares fits of the data to the power law

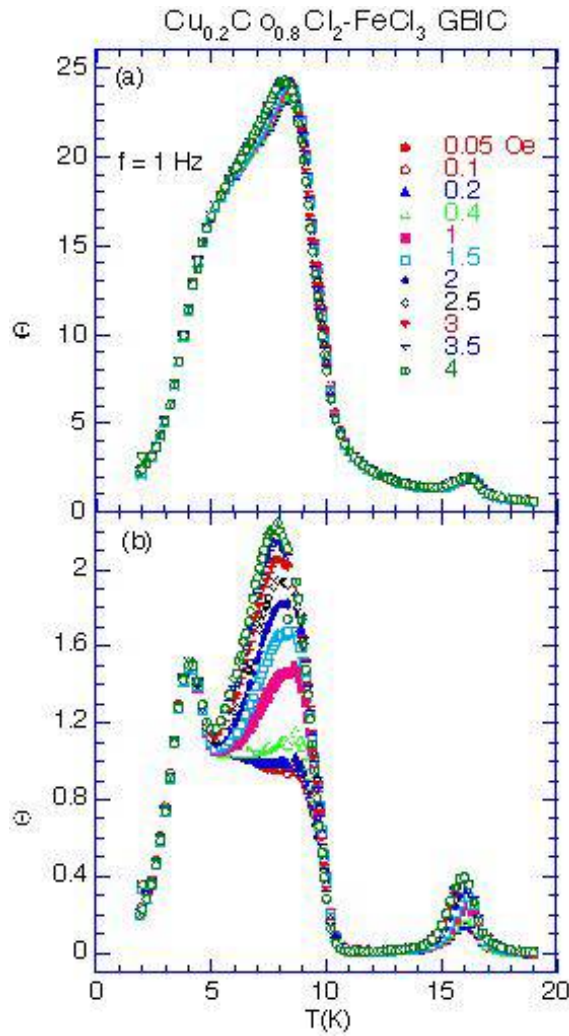


FIG. 1: T dependence of (a) $\chi'_1 = h$ and (b) $\chi''_1 = h$ at various h for $\text{Cu}_{0.2}\text{Co}_{0.8}\text{Cl}_2\text{-FeCl}_3$ GBIC. $f = 1$ Hz, $H = 0$.

form is:²⁴

$$\chi'_1 = h = \chi'_1 + 3\chi'_3 h^2 + 4 + 10\chi'_5 h^4 = 16 + \quad ; \quad (1)$$

and

$$\chi''_1 = h = \chi''_1 + 3\chi''_3 h^2 + 4 + 10\chi''_5 h^4 = 16 + \quad : \quad (2)$$

Note that for convenience we use the linear AC susceptibility χ'_0 and χ''_0 instead of χ'_1 and χ''_1 . In Figs. 1 (a) and (b) we show the T dependence of the dispersion $\chi'_1 = h$ and the absorption $\chi''_1 = h$ at $f = 1$ Hz. The different curves correspond to different amplitudes of the AC field, where h is varied between 1 mOe and 4.2 Oe. The susceptibility $\chi'_1 = h$ and $\chi''_1 = h$ are independent of h for $h < h_0$ within experimental error, where $h_0 \approx 0.1$ Oe, implying that $\chi'_1 = h$ and $\chi''_1 = h$ coincide with the linear susceptibilities χ'_0 and χ''_0 , respectively. Note that $\chi''_1 = h$ shows a sharp peak at 4 K, which is almost independent of h . This sharp peak is associated with the transition between the FM and RSG phases: $T_{\text{RSG}} = 3.5$ K.

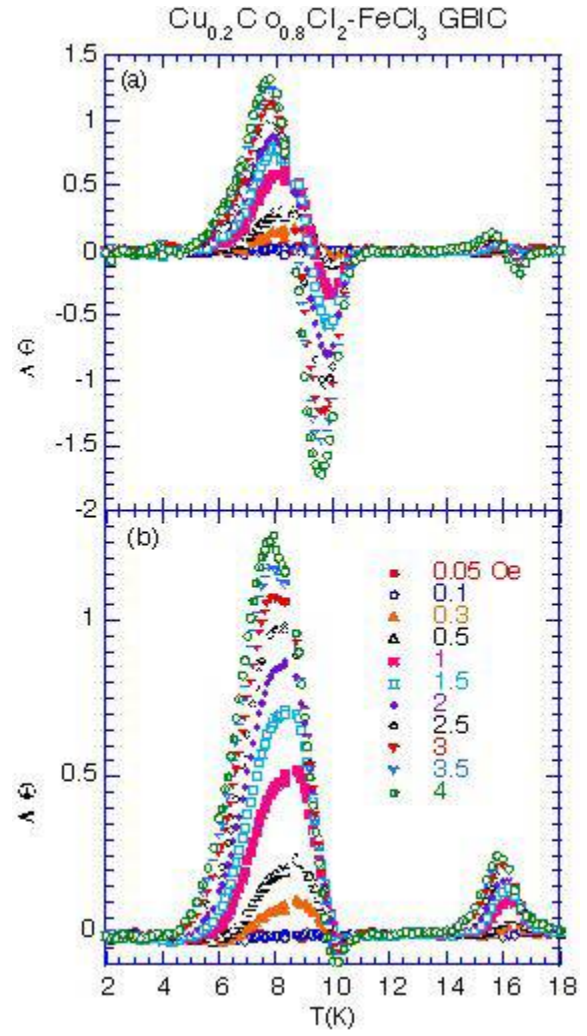


FIG. 2: T dependence of (a) $(\chi'_1 = h)$ and (b) $(\chi''_1 = h)$ at various h . $f = 1$ Hz, $H = 0$. $(\chi'_1 = h)$ is defined by the difference between $\chi'_1 = h$ at $h > 30$ mOe and $\chi'_1 = h$ at $h = 30$ mOe. $(\chi''_1 = h)$ is defined by the difference between $\chi''_1 = h$ at $h > 30$ mOe and $\chi''_1 = h$ at $h = 30$ mOe.

In Figs. 2 (a) and (b) we show the T dependence of $(\chi'_1 = h)$ and $(\chi''_1 = h)$ at various h , where $(\chi'_1 = h)$ and $(\chi''_1 = h)$ are defined as the differences between $\chi'_1 = h$ and $\chi''_1 = h$ at $h > 30$ mOe and those at $h = 30$ mOe, respectively: $(\chi'_1 = h) = 3\chi'_3 h^2 + 4 + 10\chi'_5 h^4 = 16 +$ and $(\chi''_1 = h) = 3\chi''_3 h^2 + 4 + 10\chi''_5 h^4 = 16 +$. The differences $(\chi'_1 = h)$ and $(\chi''_1 = h)$ are strongly dependent on h . The difference $(\chi'_1 = h)$ has two local maxima at 16.2 K (15.8 K) and 8.6 K (7.8 K), and a local minimum at 10.3 K (10.1 K) at $h = 1$ Oe ($h = 4$ Oe). In contrast, $(\chi''_1 = h)$ has two local maxima at 15.8 K (15.6 K) and 8.3 K (7.8 K), and two local minima at 9.9 K (9.5 K) and 16.6 K (16.5 K) at $h = 1$ Oe ($h = 4$ Oe). In summary, the positions of the local maxima and minima shift to low-T side as h increases.

In Figs. 3 and 4 we show the plot of $(\chi''_1 = h)$ and $(\chi'_1 = h)$ as a function of h^2 near T_c (≈ 9.7 K) and T_h

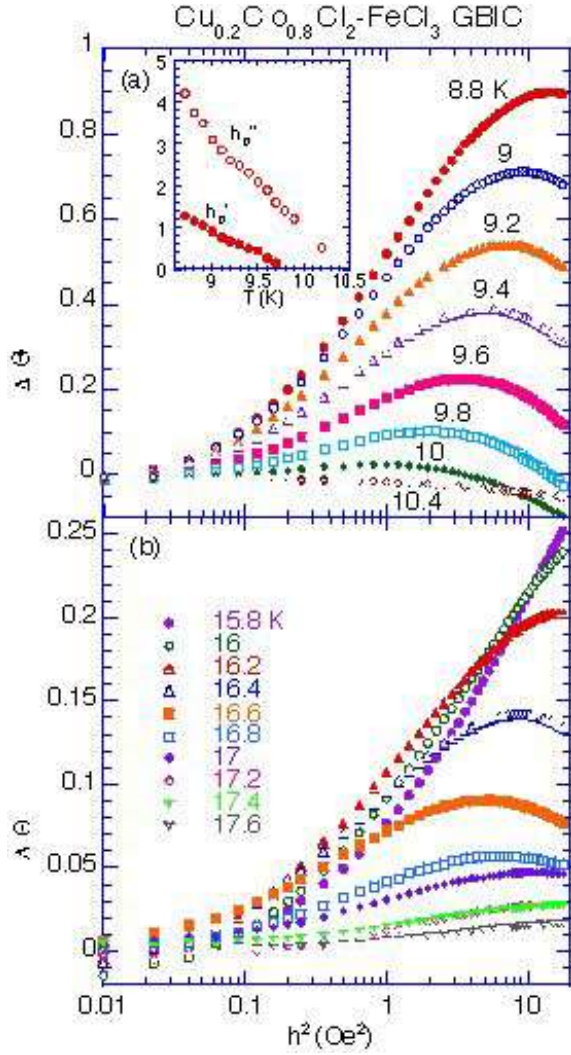


FIG. 3: (a) and (b) h^2 dependence of $\chi''(h)$ at various T . $f = 1$ Hz. The inset of (a) shows the T dependence of the peak field h_p^0 for $\chi''(h)$ and h_p^0 for $\chi'(h)$.

(≈ 16 K), respectively. Both $\chi''(h)$ and $\chi'(h)$ are strongly dependent on h^2 in these limited temperature regions. A linear increase of $\chi''(h)$ and $\chi'(h)$ with h^2 at low h indicates a positive sign of χ''_3 and χ'_3 . We find a peak in $\chi''(h)$ [$\chi'(h)$] at a peak field h_p^0 [h_p^0], which shifts to the low- h side with increasing T . The fields h_p^0 and h_p^0 are defined as $d(\chi''(h))/dh = 0$ and $d(\chi'(h))/dh = 0$, respectively: $h_p^0 = 3\chi''_3/(5\chi''_5)$ and $h_p^0 = 3\chi'_3/(5\chi'_5)$. The existence of h_p^0 and h_p^0 indicates a negative sign of χ''_5 and χ'_5 . In the inset of Fig. 3(a), we show the T dependence of h_p^0 and h_p^0 . The peak fields h_p^0 and h_p^0 , which decrease with increasing T , tend to reduce to zero around 9.8 and 10.4 K, respectively.

The least squares fits of the data ($\chi''(h) \propto h^2$ and $\chi''(h) \propto h^4$) at each T for $30 \text{ mOe} < h < 0.7 \text{ Oe}$ to Eqs. (1) and (2) yield the values of χ''_1 , χ''_3 , χ''_5 , χ''_7 , and χ''_9 . Figure 5 shows the T dependence of χ''_3 , χ''_5 , χ''_7 , and χ''_9 thus obtained. The nonlinear susceptibility χ''_3 at $f = 1$

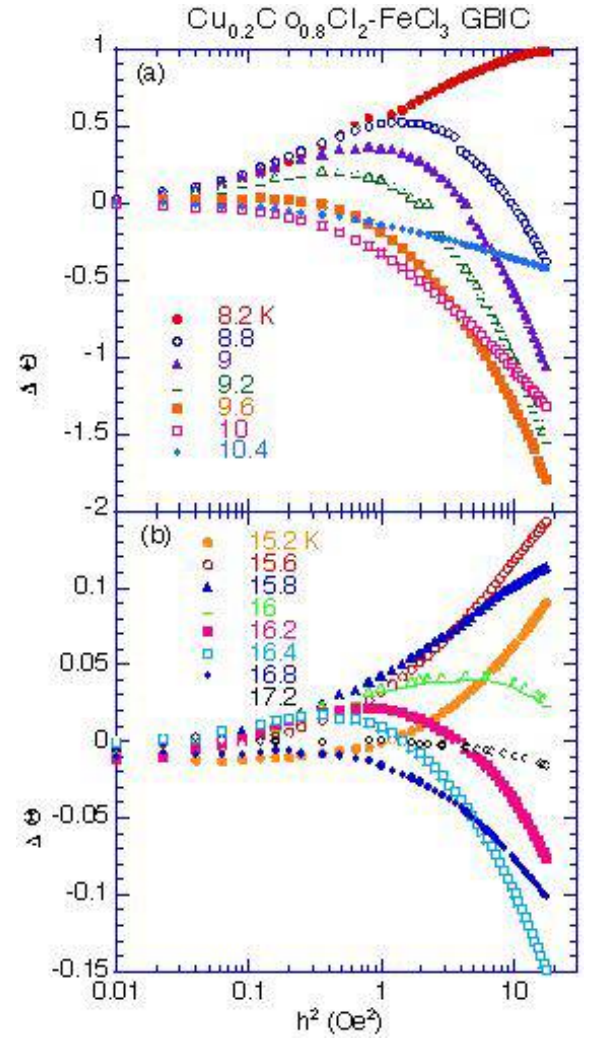


FIG. 4: (a) and (b) h^2 dependence of $\chi''(h)$ at various T . $f = 1$ Hz.

Hz shows a positive peak at 16.0 K, a negative local minimum at 10.2 K, and two positive peaks at 8.8 and 8.3 K. The sign of χ''_3 changes from negative to positive at 9.65 K and from positive to negative at 4.0 K with decreasing T . No anomaly is observed below 4 K. In contrast, χ''_5 at $f = 1$ Hz exhibits a negative local minimum at 16.0 K, a positive peak at 10.2 K, and two negative peaks at 9.0 K and 8.3 K. The sign of χ''_5 changes from positive to negative at 4.0 K with decreasing T . We note that the T dependence of χ''_3 around 10 K in our system is similar to that in stage-2 CoCl_2 GBIC which magnetically behave like a quasi-2D ferromagnet with an extremely weak antiferromagnetic interplanar exchange interaction.²⁴ In stage-2 CoCl_2 GBIC, χ''_3 exhibits a negative local minimum at 10.5 K, becomes positive below 10.2 K, and shows a positive peak below the upper critical temperature T_{Cu} .

The nonlinear susceptibility χ''_5 shows a positive peak at 16.2 K, a negative local minimum at 11.0 K, and a positive peak at 8.7 K. The sign of χ''_5 changes from negative to positive at 9.9 K and from positive to negative

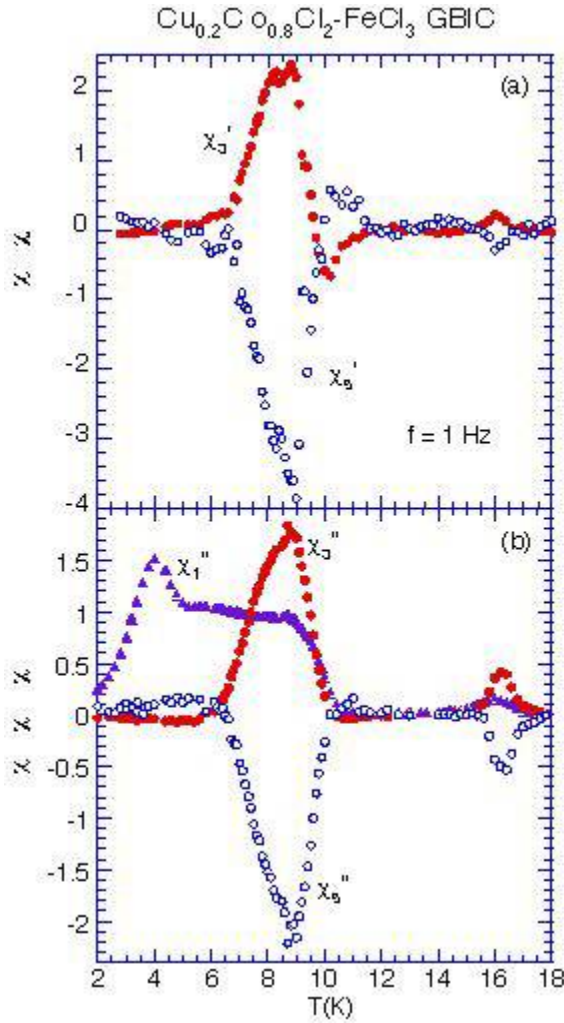


FIG. 5: (a) T dependence of χ'_3 and χ''_3 , where the units of χ'_{2n+1} are $\text{emu}/(\text{av mol Oe}^{2n+1})$. $f = 1 \text{ Hz}$. (b) T dependence of $d\chi'_1/dT$, $d\chi'_3/dT$, and $d\chi''_5/dT$, where the units of χ'_{2n+1} are $\text{emu}/(\text{av mol Oe}^{2n+1})$.

at 5.7 K with decreasing T. In contrast, χ''_5 shows a negative local minimum at 16.4 K, a positive peak at 11.0 K, and a negative peak at 9.0 K. The sign of χ''_5 changes from negative to positive at 6.5 K with decreasing T.

Here we discuss the T dependence of χ'_3 . Basically the singularity of χ'_3 could reflect the breaking of spatial magnetic symmetry. The sign of χ'_3 is negative for the PM phase and the SG phase and positive for the FM phase. Thus the critical temperatures T_c for the PM-FM transition and T_{RSG} for the FM-RSG transition could be defined as temperatures at which the sign of χ'_3 changes. Using this definition, in fact we find 9.65 K as T_c and 4.0 K as T_{RSG} at $f = 1 \text{ Hz}$ for our system. Similar behaviors have been reported in other reentrant ferromagnets. Sato and Miyako²⁵ have reported that the sign of χ'_3 in $(\text{Pd}_{0.9966}\text{Fe}_{0.0034})_{0.95}\text{Mn}_{0.05}$ changes from negative to positive at T_c . Sato et al.⁷ have shown that the sign of χ'_3 in $\text{Ni}_{0.77}\text{Fe}_{0.23}\text{Mn}_{0.22}$ changes from positive to nega-

tive at T_{RSG} : χ'_3 has a small negative local minimum near T_{RSG} .

B. Linear AC susceptibility: χ' and χ''

Figures 6(a) and (b) show the T dependence of the linear AC susceptibility χ' and χ'' below 12 K at $h = 50 \text{ mOe}$, where $\chi'_1 = h = \chi'_1 = \chi'$ and $\chi''_1 = h = \chi''_1 = \chi''$. The absorption χ'' at $f = 0.01 \text{ Hz}$ shows a relatively sharp peak at 3.69 K. This peak shifts to the high-T side with increasing f : 5.10 K at $f = 1 \text{ kHz}$. In contrast, the derivative $d\chi''/dT$ at $f = 0.01 \text{ Hz}$ shows two negative local minima at 4.0 K corresponding to T_{RSG} and 10.0 K corresponding to T_c . The local minimum $d\chi''/dT$ vs T at 4.0 K shifts to the high-T side with increasing f , while the local minimum at 10.0 K does not shift with increasing f .

Figures 6(c) and (d) show the T dependence of χ' and χ'' around T_h at $h = 500 \text{ mOe}$, where $\chi'_1 = h = \chi'$ and $\chi''_1 = h = \chi''$. The dispersion χ' at $f = 0.01 \text{ Hz}$ shows peaks at 16.2 K and 8.35 K. The peak at 16.2 K slightly shifts to the high-T side with increasing f : 16.4 K at $f = 1 \text{ kHz}$. Another peak at 8.35 K does not shift with increasing f . The dispersion χ'' at $f = 0.01 \text{ Hz}$ has an inflection point at 3.5 K corresponding to the positive peak of $d\chi''/dT$, and another inflection point at 9.7 K corresponding to the negative local minimum of $d\chi''/dT$. The inflection point at 3.5 K shifts to the high-T side with increasing f .

Here we assume that the singular behavior of χ'' around 4 K is due to the critical slowing down associated with the FM-RSG transition. Either the peak temperatures of χ'' vs T and T vs χ'' or the local minimum temperature of $d\chi''/dT$ vs T around 4 K coincide with a spin freezing temperature T_f at a relaxation time $(\tau = 1)$. The relaxation time can be described by²⁶

$$\tau = (T_f - T_{\text{RSG}})^{-x}; \quad (3)$$

where $x = z/\nu$, z is the dynamic critical exponent, ν is the critical exponent of the spin correlation length, and τ is the characteristic time. In Fig. 7 we show the T dependence of τ thus obtained for $d\chi''/dT$, T vs χ'' (figure of T vs χ'' is not shown), and χ'' . The least squares fits of the data of τ vs T yield $x = 8.5 \pm 1.8$, $T_{\text{RSG}} = 3.45 \pm 0.31 \text{ K}$, and $\tau = (4.77 \pm 0.10) \times 10^{-6} \text{ sec}$ for the local minimum temperature of $d\chi''/dT$ vs T, $x = 12.3 \pm 1.7$, $T_{\text{RSG}} = 2.90 \pm 0.26 \text{ K}$, and $\tau = (1.49 \pm 0.05) \times 10^{-5} \text{ sec}$ for the peak temperature of T vs χ'' , and $x = 16.6 \pm 1.8$, $T_{\text{RSG}} = 2.27 \pm 0.25 \text{ K}$, and $\tau = (4.67 \pm 0.10) \times 10^{-3} \text{ sec}$ for the peak temperature of χ'' vs T. The value of x for χ'' vs T and T vs χ'' is unphysically large. In contrast, the value of x for $d\chi''/dT$ vs T is on the same order as that ($x = 7.9$) reported by Jonason et al.⁴ for the FM-RSG transition of $(\text{Fe}_{0.20}\text{Ni}_{0.80})_{0.75}\text{P}_{0.16}\text{B}_{0.09}\text{A}_{0.06}$. A relatively good agreement between the value of x for $\text{Cu}_{0.2}\text{Co}_{0.8}\text{Cl}_2\text{-FeCl}_3 \text{ GBIC}$ and the value predicted by Ogilski²⁷ for the

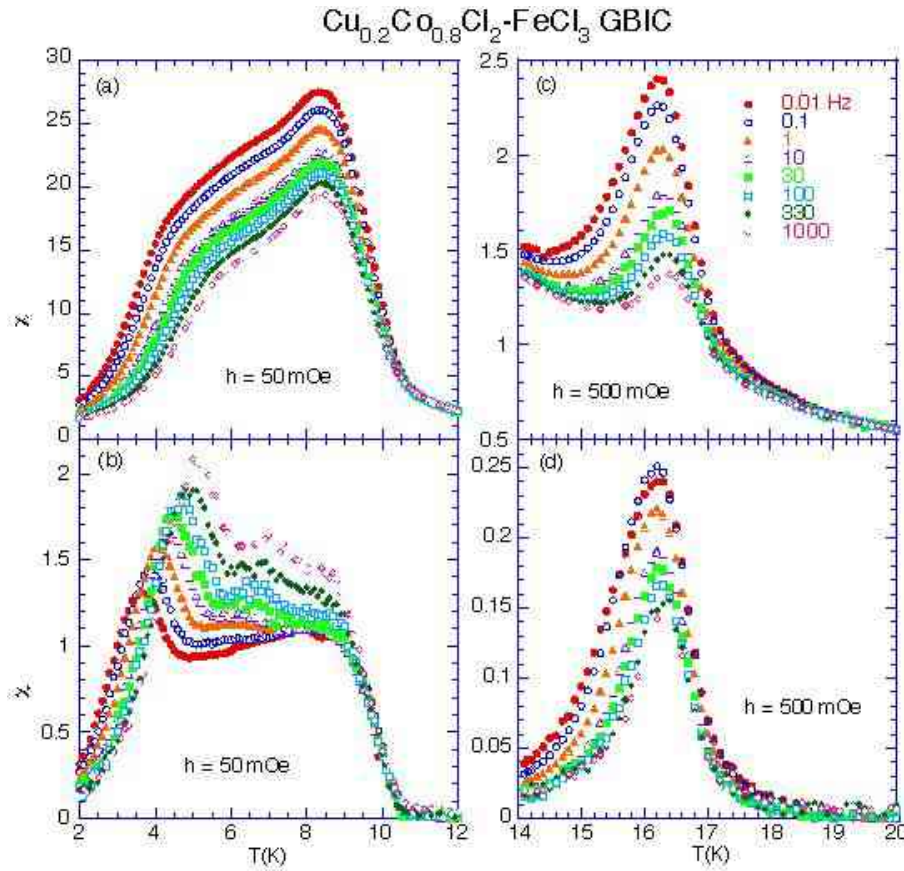


FIG. 6: (a), (b) T dependence of χ' ($= \chi'_{01}$) and χ'' ($= \chi''_{01}$) at various f . $h = 50$ mOe. $H = 0.2$ T. $T = 12$ K. (c), (d) T dependence of χ' ($= \chi'_{01}$) and χ'' ($= \chi''_{01}$) at various f . $h = 500$ mOe. $H = 0.14$ T. $T = 20$ K.

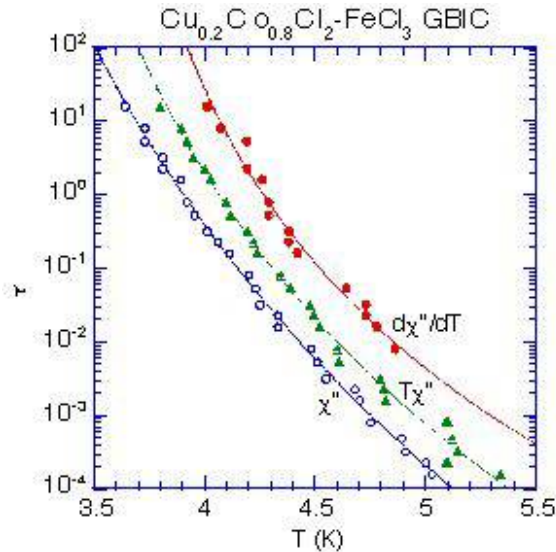


FIG. 7: T dependence of the relaxation time τ which is determined from the f dependence of peak temperature of χ'' vs T , $T\chi''$ vs T , and $d\chi''/dT$ vs T . The solid lines denote the least-squares fit of the data to Eq.(3).

3D J Ising SG ($x = 7.9 \pm 1.0$), suggests that the FM - RSG transition in our system is dynamically similar to an ordinary PM - SG transition. Note that the value of $d\chi''/dT$ vs T is much larger than a typical value of microscopic relaxation time τ_0 (typically $10^{10} - 10^{12}$ sec). Such a large value of τ has been also reported by Klemann et al.²⁸ for $\text{Co}_{80}\text{Fe}_{20}/\text{Al}_2\text{O}_3$ multilayers: $\tau = (6.7 \pm 0.4) \times 10^7$ sec and $x = 10.0 \pm 3.6$. The large τ suggests that the PM clusters play a significant role in the FM - RSG transition. In the random - field picture,⁶ the FM phase consists of the FM region with a longer relaxation time and the PM clusters with a shorter relaxation time. On decreasing T toward T_{RSG} , the thermal fluctuations of the spins in the PM clusters become slower. The molecular field of the slow PM spins acting as random magnetic field causes breakups of the FM network into finite-sized clusters. It is predicted that the following dynamic scaling equation is valid for the normal SG phase:²⁹ $T\tau^\gamma = \tau_0^\gamma f^x$ (!), where f (!) is a scaling function of f and is assumed to take a maximum at $f = \text{constant}$. The value γ ($= x$) is a critical exponent, where x is a critical exponent of the order parameter. The curve of $T\tau^\gamma$ vs T exhibits a peak, which shifts to the high- T side as f increases. The peak height of $T\tau^\gamma$ increases with increasing f . The least squares fit of the

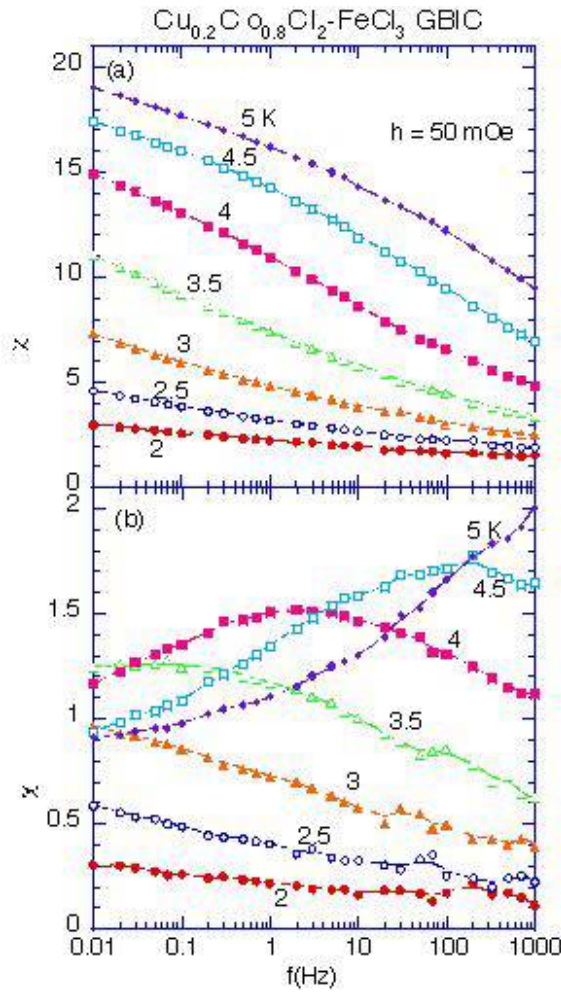


FIG. 8: f dependence of (a) χ'' and (b) χ'' at various T . $h = 50$ mOe.

data for the peak height of χ'' vs f (for $0.01 < f < 1000$ Hz) to the form of $(\chi''/f)^y$ yields $y = 0.066 \pm 0.001$. Then the value of $\alpha = xy$ is estimated as $\alpha = 0.57 \pm 0.10$, where $x = 8.5 \pm 1.8$. This value of α is similar to that ($\alpha = 0.54$) for $\text{Fe}_{0.5}\text{Mn}_{0.5}\text{TiO}_3$.³⁰ In summary, the nature of the FM-RSG transition is similar to that of the normal PM-SG transition. The PM clusters for the FM-RSG transition play the same role as individual spins for the PM-SG transition.

Figures 8(a) and (b) show the f dependence of $\chi''(T; f)$ and $\chi''(T; f)$ at various T in the vicinity of T_{RSG} , respectively. The absorption $\chi''(T; f)$ curves exhibit different characteristics depending on T . Above T_{RSG} , $\chi''(T; f)$ shows a peak at a characteristic frequency, shifting to the low f -side as T decreases. Below T_{RSG} , $\chi''(T; f)$ shows no peak for $f > 0.01$ Hz. It decreases with increasing f , following a power law form $(\chi''/f)^{\alpha}$. This is in contrast to the f dependence of χ'' for conventional spin glass systems such as $\text{Fe}_{0.5}\text{Mn}_{0.5}\text{TiO}_3$: χ'' increases with increasing f .²⁶ The exponent α is weakly dependent on T : $\alpha = 0.083 \pm 0.004$ at 2.5 K and $\alpha = 0.079 \pm 0.002$

at 3 K. According to the fluctuation-dissipation theorem, the magnetic fluctuation spectrum $P(\omega)$ is related to $\chi''(T; \omega)$ by $P(\omega) = 2k_B T \chi''(T; \omega)/\omega$. Then $P(\omega)$ is proportional to $\omega^{-1-\alpha}$, which is similar to $1/\omega$ character of typical spin glass. In contrast, $\chi''(T; \omega)$ decreases with increasing ω above and below T_{RSG} : χ'' exhibits a power law form $(\chi''/\omega)^{\beta}$. The exponent β is weakly dependent on T : $\beta = 0.079 \pm 0.001$ at $T = 2.5$ K and $\beta = 0.094 \pm 0.001$ at $T = 3.0$ K. The value of β agrees well with that of α . Note that α is related to β through a so called $\alpha/2$ rule: $\alpha = (\beta/2)d\chi''/d\ln\omega$ (Kramers-Kronig relation), leading to the relation $\beta = 2\alpha$.

Here we note the f dependence of χ'' above 5 K (which is not shown in Fig. 8(b)). The absorption χ'' increases with increasing f for $5 < T < 7.2$ K. A newly small peak is added around $f = 2$ Hz for $7.3 < T < 9.2$ K. The absorption χ'' decreases with increasing f for $f > 70$ Hz and increases with further increasing f for $9.3 < T < 9.8$ K. Above 9.9 K it decreases with increasing f . We find that χ'' for $6.1 < T < 7.3$ K can be described by a power law form $(\chi''/\omega)^{\alpha}$ in the limited frequency range ($0.01 < f < 10$ Hz). The exponent α increases with increasing T : $\alpha = 0.04 \pm 0.01$ at 6.1 K, 0.081 ± 0.02 at 6.7 K, and 0.12 ± 0.01 at 7.2 K.

$$C = \chi_{\text{FC}} - \chi_{\text{ZFC}}, \text{ and } \chi_{\text{FC}} = \chi_{\text{ZFC}} + C$$

Figures 9 shows the T dependence of χ_{FC} and χ_{ZFC} at various H , where H is applied along the c plane which is perpendicular to the c axis. It is strongly dependent on H . The susceptibility χ_{FC} at $H = 0.5$ Oe decreases with increasing T . It has inflection points at $T = 16.4$, 9.70, and 4.0 K where $d\chi_{\text{FC}}/dT$ exhibits negative local minima. These temperatures correspond to the transition temperatures T_h , T_c , and T_{RSG} . In contrast, χ_{ZFC} at $H = 0.5$ Oe exhibits two peaks at 16.2 and 8.2 K, and an inflection point at 3.2 K where $d\chi_{\text{ZFC}}/dT$ shows a positive local maximum. The peaks of χ_{ZFC} at 8.2 and 16.2 K shifts to the low- T side with increasing H . The deviation of χ_{ZFC} at $H = 0.5$ Oe from χ_{FC} starts to occur at temperatures above 18 K. The peak of χ_{ZFC} at T_h is very sensitive to the application of H . It shifts to the low- T side with increasing H and disappears above 50 Oe.

Figure 10 shows the T dependence of the difference $\chi_{\text{FC}} - \chi_{\text{ZFC}}$ at various H . The difference has three inflection points at T_h , T_c , and T_{RSG} , where $d(\chi_{\text{FC}} - \chi_{\text{ZFC}})/dT$ exhibits negative local minima: 16.2 K (T_h), 9.60 K (T_c), and 3.40 K (T_{RSG}). The T dependence of $\chi_{\text{FC}} - \chi_{\text{ZFC}}$ shown in Fig. 10 is very different from standard one observed in many reentrant ferromagnets, where $\chi_{\text{FC}} - \chi_{\text{ZFC}}$ reduces to zero at T_{RSG} . Typical examples of χ_{ZFC} vs T and χ_{FC} vs T have been reported for $\text{CdCr}_{2-x}\text{In}_{2x}\text{S}_4$,¹² $\text{Au}_{85}\text{Fe}_{15}$,³¹ $\text{Ni}_{47}\text{Mn}_{23}$,³² and $(\text{Fe}_{0.90}\text{Co}_{0.05}\text{Ni}_{0.05})_2\text{P}$.³³ Both inflection points of $\chi_{\text{FC}} - \chi_{\text{ZFC}}$ at $T_c(H)$ and $T_h(H)$ become less pronounced with increasing H . Only an inflection point at $T_{\text{RSG}}(H)$ sur-

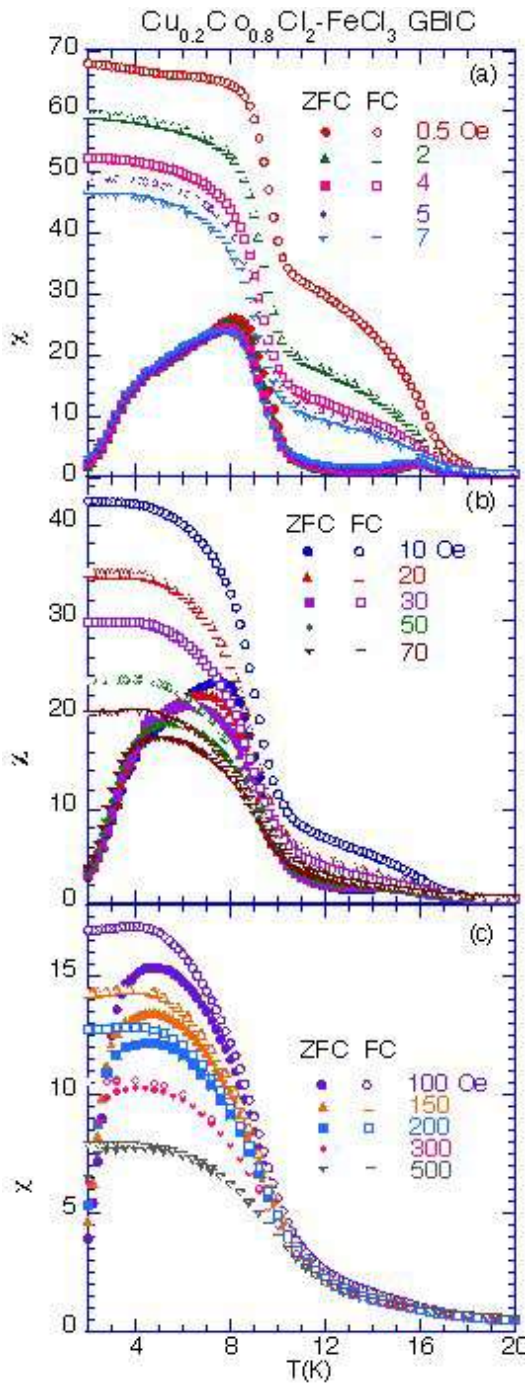


FIG. 9: (a)-(c) T dependence of M_{ZFC} and M_{FC} at various H . H is in Oe.

exists for $H = 100$ Oe. Note that the inflection point at $T_{RSG}(H)$ shifts to the low- T side with increasing H : 2.8 K at $H = 100$ Oe. The H dependence of $T_{RSG}(H)$ will be discussed in Sec. III E.

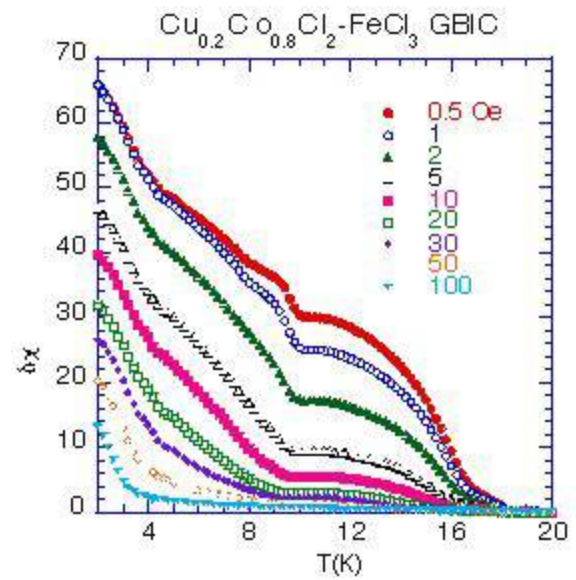


FIG. 10: T dependence of $(M_{FC} - M_{ZFC})$ at various H . The value of M_{ZFC} is derived from Fig. 9.

D. M_{IR} and M_{TR} in the IR and TR states

We have measured the magnetization M in the ZFC, FC, IR (isothermal remnant), and TR (thermoremanent) states in the case of $H = 5$ and 15 Oe, as a function of T . This magnetization M is slightly different from usual M , because of different methods of measurements. The measurements of M were carried out as follows. First the sample was quenched from 298 to 1.9 K at $H = 0$. Then H ($= 5$ or 15 Oe) was applied. The measurements of M_{ZFC} and M_{IR} were done with increasing T from 1.9 to 20 K. At each T , M_{ZFC} was measured at the same H and then M_{IR} was measured 100 sec later after the field was changed from H to 0 Oe. Second, the sample was annealed at 100 K for 1200 sec at H . The measurements of M_{FC} and M_{TR} were done with decreasing T from 20 to 1.9 K. At each T , M_{FC} was measured at H and then M_{TR} was measured 100 sec later after the field was changed from H to 0 Oe.

Figure 11 shows the T dependence of M_{ZFC} , M_{IR} , M_{FC} , and M_{TR} , $M = (M_{FC} - M_{ZFC})$, $M = (M_{TR} - M_{IR})$ in the case of $H = 5$ and 15 Oe. Note that the T dependence of M_{FC} is not exactly the same as that of M_{FC} , because of the difference in the method of field cooling. While M_{FC} shown in Fig. 9 (a) increases with decreasing T , M_{FC} shows a peak at 7.5 K between T_c and T_{RSG} and an inflection point at T_{RSG} where dM_{FC}/dT exhibits a positive local maximum. This result is indicative of a non-uniformity in the FM phase: frustrated spins coexists with ferromagnetically aligned spins.

The T dependence of M_{TR} is exactly the same as that of M . The magnetization M_{TR} (measured at $H = 0$) in the case of $H = 5$ Oe shows a broad peak around 10.6 K just above T_c , and reduces to zero at T_h . In contrast,

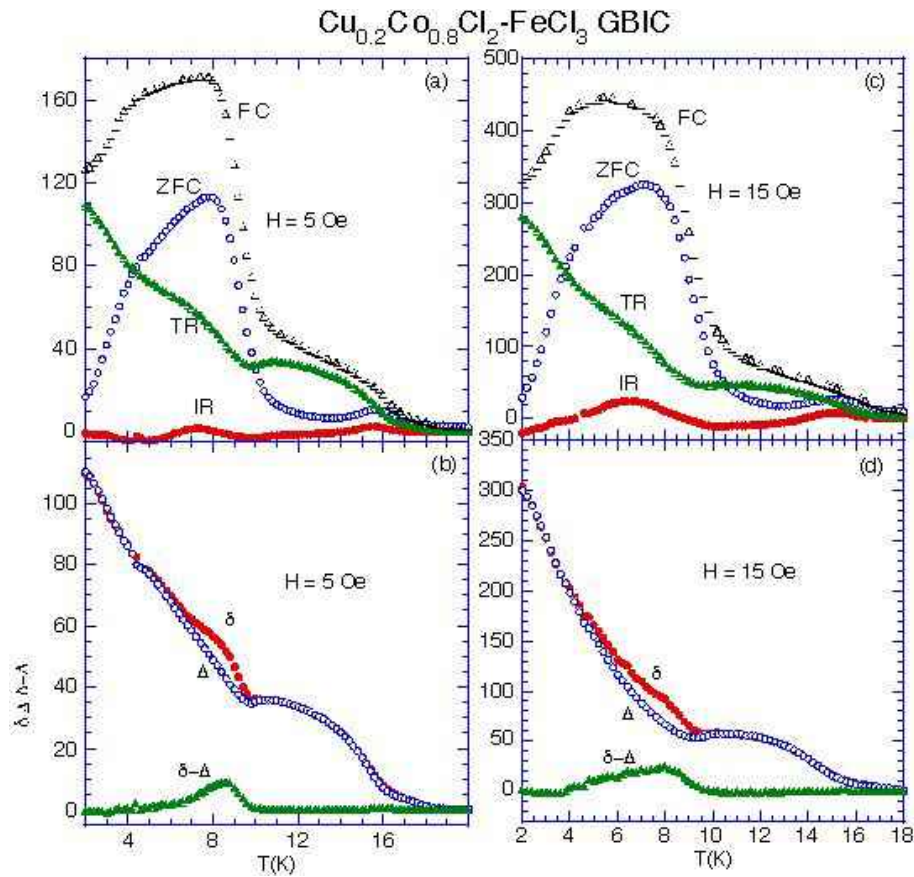


FIG. 11: T dependence of M_{ZFC} , M_{FC} , M_{IR} , M_{TR} , $M_{\text{FC}} - M_{\text{ZFC}}$ and $M_{\text{TR}} - M_{\text{IR}}$. $H \parallel c$. (a), (b) $H = 5$ Oe and (c), (d) $H = 15$ Oe. The definition of M for each state is given in the text.

M_{IR} is much smaller than M_{TR} . The difference M is different from M between T_{RSG} and T_{C} . In fact, the difference ($M_{\text{TR}} - M_{\text{IR}}$) is larger than zero only between T_{RSG} and T_{C} and near T_{h} .

As far as we know, there has been only one report on M_{TR} (measured by a conventional method) in a reentrant ferromagnet $(\text{Fe}_{0.90}\text{Co}_{0.05}\text{Ni}_{0.05})_2\text{P}$.³³ M_{TR} was measured as T increases after cooling down the system to the lowest T in the presence of H (FC cooling), annealing at T at a waiting time t_w , and then reducing H to zero. The magnetization M_{TR} shows a local minimum at T_{RSG} and a broad peak between T_{RSG} and T_{C} . It reduces to zero at T_{C} with increasing T .

E. H - T phase diagram

We have measured the T dependence of χ'' and χ''' at various H for $f = 100$ Hz and 0.1 Hz, where H ($0 < H \leq 2$ kOe) is applied along the c plane perpendicular to the c -axis. Figures 12 shows the T dependence of χ'' and χ''' at various H for $f = 100$ Hz. The AC field h ($= 50$ mOe) was used for $1.9 \leq T \leq 12$ K and a larger h ($= 500$ mOe) was used for $14 \leq T \leq 19$ K. The peak of χ'' and the shoulder of χ''' around T_{C} disappears for $H \geq 50$ Oe, and

the peaks of χ'' and χ''' around T_{h} disappears for $H \geq 7$ Oe. The peak of χ''' around T_{RSG} shifts to the low T -side with increasing H for $0 \leq H \leq 1$ kOe. The peak of χ''' around T_{h} also shifts to the low T -side with increasing H for $0 \leq H \leq 7$ Oe. In Figs. 13(a) and (b) we show the H - T diagrams around T_{RSG} and T_{h} , respectively. Here the temperature (denoted as $T_{\text{f}}(H)$) of negative local minimum of $d\chi''/dT$ vs T at 0.1 Hz (data are not shown) is plotted as a function of H . For comparison, we also show the H dependence of the negative local minimum temperatures of $d\chi'/dT$ vs T and the peak temperatures of χ''' vs T at $f = 0.1$ and 100 Hz. These lines are away from the line $T_{\text{f}}(H)$. The least squares fit of the data of the line $T_{\text{f}}(H)$ for $0 \leq H \leq 600$ Oe to

$$H = H_0 [1 - T_{\text{f}}(H)/T_g]^p; \quad (4)$$

yields parameters $p = 1.55 \pm 0.13$, $T_g = 4.26 \pm 0.11$ K, and $H_0 = (2.6 \pm 0.3)$ kOe. Note that the value of T_g ($= 4.26$ K) is larger than that of T_{RSG} ($= 3.45 \pm 0.31$ K). The value of exponent p is close to that ($p = 1.50$) for the de Almeida-Thouless (AT) line.³⁴ In the mean field picture, the AT line separates the replica-symmetry (FM) phase from the replica-symmetry-breaking (RSB) phase in the (H, T) line.

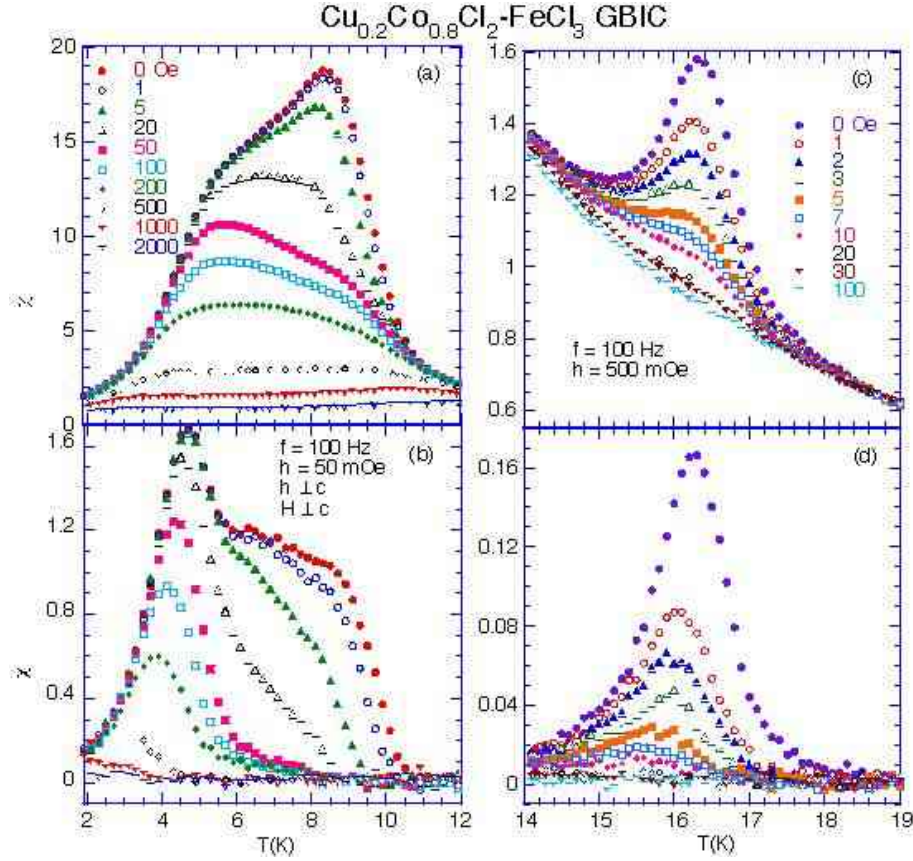


FIG. 12: T dependence of (a) M and (b) M'' at various H . H is applied along the c plane perpendicular to the graphene plane ($H \parallel c$). $f = 100$ Hz, $h = 50$ mOe, $h \parallel c$, $H \perp c$. (c) M and (d) M'' at various H . $H \parallel c$, $f = 100$ Hz, $h = 500$ mOe, $h \parallel c$. $14 < T < 19$ K.

F. Aging: $M_{ZFC}(t; T)$, $M''(t; T)$, and $M'(t; T)$

In order to reveal a possible aging phenomenon in the RSG phase and FM phase, we have studied time (t) dependence of the zero-field cooled magnetization M_{ZFC} . First the system was cooled from 100 K to T in the absence of H , where the remnant magnetic field is less than 3 mOe. The system was kept at T for a wait time t_w ($= 2.0 \times 10^3$ sec). A DC magnetic field ($H = 10$ Oe) was applied at $t = 0$. The magnetization (M_{ZFC}) was measured as a function of elapsed time after the field application. Figure 14 shows the t dependence of $M_{ZFC}(t)$ at $T = 3$ and 7 K. The corresponding relaxation rate $S(t)$ [$= (1/H) dM_{ZFC}(t)/dt = d \ln t$] is shown in Fig. 15 as a function of t for each T . The relaxation rate $S(t)$ at $T = 3$ K has a peak around $t_p = 4 \times 10^3$ sec which is larger than t_w . Note that the inflection point of M_{ZFC} corresponds to the peak of $S(t)$. At $T = 4$ K, $S(t)$ shows a very flat plateau between 3.2×10^3 and 10^4 sec, in addition to a small peak at $t_p = 1.1 \times 10^4$ sec. Such an aging behavior does not end at T_{RSG} , but sustains into the FM phase. The relaxation rate $S(t)$ has a peak at a time shorter than t_w for $5 < T < 7$ K: $t_p = 1.6 \times 10^3$ sec at $T = 5$ K, 1×10^3 sec at 6 K, and 1.3×10^3 sec at 7 K. The

TABLE I: Least squares fitting parameters of $M_{ZFC}(t)$ to the power law form given by Eq.(6). $H = 10$ Oe, $t_w = 2.0 \times 10^3$ sec. The values of M_{FC} and M_{ZFC} are obtained from Fig. 9(b) at $H = 10$ Oe. M_1^0, M_2^0, M_{FC} and M_{ZFC} are in the units of emu/av mol.

T (K)	a	b	M_1^0	M_2^0	M_{FC}	M_{ZFC}
5	0.015	0.001	461.6	290.3	414.4	187.1
6	0.035	0.001	296.0	99.0	399.8	214.6
7	0.030	0.001	292.8	82.4	374.1	231.1
8	0.059	0.001	232.4	26.6	327.3	229.4
9	0.145	0.005	140.6	6.0	221.5	155.6

peak time t_p is equal to is 2.1×10^3 sec at 8 K and 1.8×10^3 sec at 9 K, which are close to t_w . Similar behavior is observed in the FM phase of $(\text{Fe}_{0.20}\text{Ni}_{0.80})_{75}\text{P}_{16}\text{B}_6\text{A}_{13}$ by Jonason et al.^{4,5}: $S(t)$ has a peak around t_w ($= 100 - 10^4$ sec).

The relaxation rate $S(t)$ clearly shows a crossover between two asymptotic relaxation regimes: the peak time t_p in the RSG phase is much longer than that in the FM phase under the same value of t_w . The FM phase of our system is chaotic in a similar way as the RSG

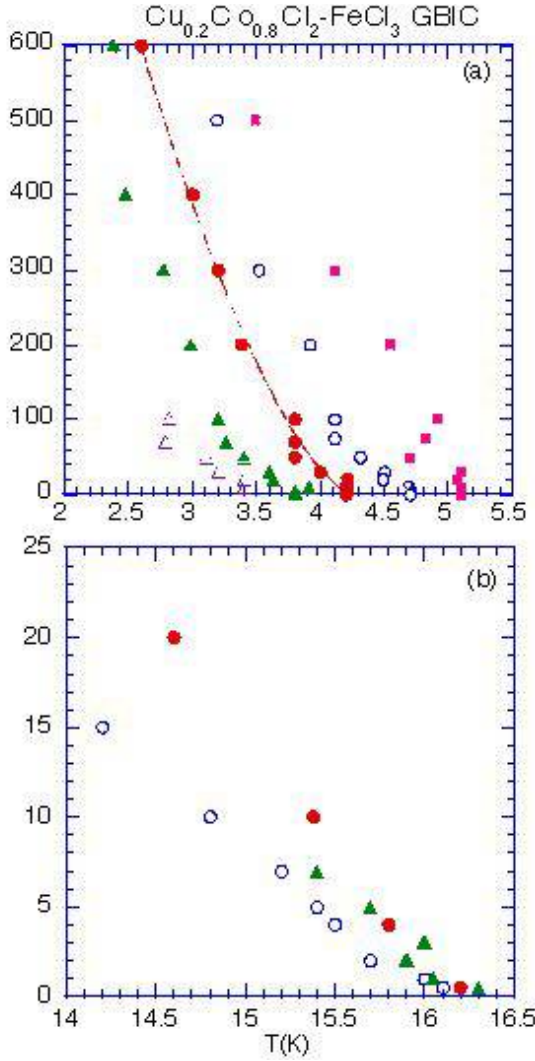


FIG. 13: (a) H - T phase diagram near T_{RSG} : for each H the local minimum temperatures of d^0/dT vs T at $f = 0.1$ Hz (○) and at 100 Hz (△), and d^0/dT vs T (□), and the peak temperatures of d^0 vs T at 0.1 Hz (●) and 100 Hz (▲). The solid line denotes the least squares fitting curve (see the text for detail). (b) H - T phase diagram near T_h : for each H the local minimum temperature of d^0/dT vs T (○), and the peak temperatures of M_{ZFC} vs T (●) and d^0 vs T at 100 Hz (▲).

phase. This is in contrast to the nonfrustrated nature of regular FM phase. The relaxation mechanism in the FM phase is different from that in the RSG phase in our system. The relaxation of $M_{ZFC}(t)$ at $T = 3$ and 4 K is described by the superposition of a stretched exponential and a constant.³⁵

$$M_{ZFC}(t) = M_1 + M_2 \exp[-(t/\tau_M)^{1/n}]; \quad (5)$$

where τ_M is a relaxation time, M_1 and M_2 are constants, the exponent $n = 0$ corresponds to the Debye, single time-constant exponential relaxation and $n = 1$ corresponds to t -independent M_{ZFC} . The least squares fit of

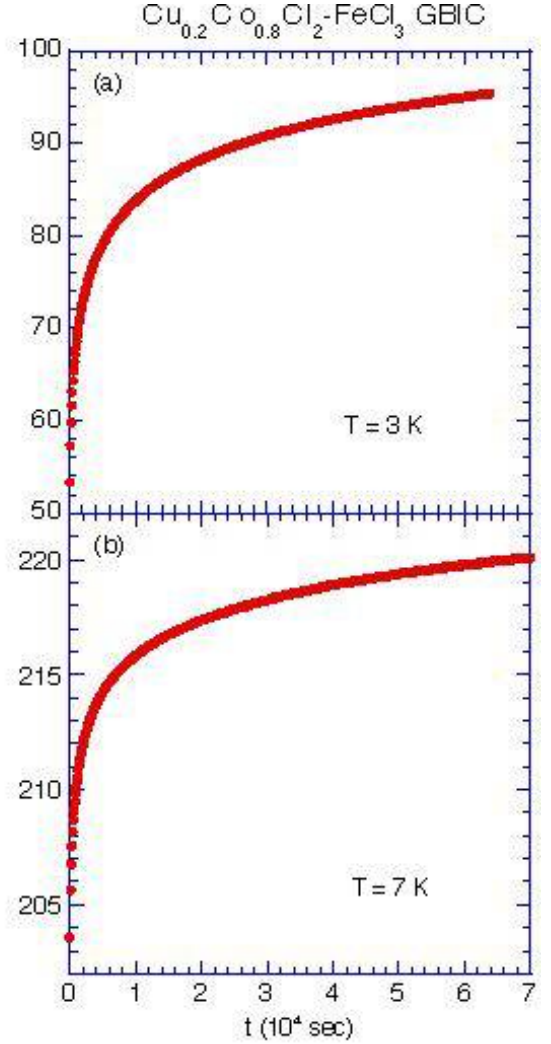


FIG. 14: t dependence of M_{ZFC} at $T = 3$ and 7 K. $\tau_w = 2.0 \times 10^3$ sec. $H = 10$ Oe. $H \parallel c$. See the detail of the measurement and the definition of $t = 0$ in the text.

the data to Eq.(5) yields $n = 0.761 \pm 0.002$, $M_1 = (6.20 \pm 0.05) \times 10^3$ sec, $M_1 = 108.72 \pm 0.17$ (emu/av mol), $M_2 = 76.93 \pm 0.53$ (emu/av mol) for $T = 3$ K, and $n = 0.819 \pm 0.001$, $\tau_M = (6.49 \pm 0.04) \times 10^3$ sec, $M_1 = 171.53 \pm 0.11$ (emu/av mol), $M_2 = 70.28 \pm 0.33$ (emu/av mol) for $T = 4$ K. In contrast, the relaxation of $M_{ZFC}(t)$ for $5 \leq T \leq 9$ K can be well described by a simple power law form and a constant:^{35,36}

$$M_{ZFC}(t) = M_1^0 + M_2^0 t^a; \quad (6)$$

where a is the exponent, and M_1^0 and M_2^0 are constant magnetizations. The magnetization M_1^0 is the saturation value which M_{ZFC} reaches in the limit of $t \rightarrow \infty$. The least squares fit of the data to Eq.(6) yields the parameters listed in Table I. The exponent a is roughly on the same order as that reported by Li et al.³⁵ for a reentrant ferromagnet $(Fe_{0.65}Ni_{0.35})_{0.882}Mn_{0.118}$ ($a = 0.088 - 0.060$ for $T_c < T < T_{RSG}$). However, the value of a in our system tends to increase with increasing T between T_{RSG}

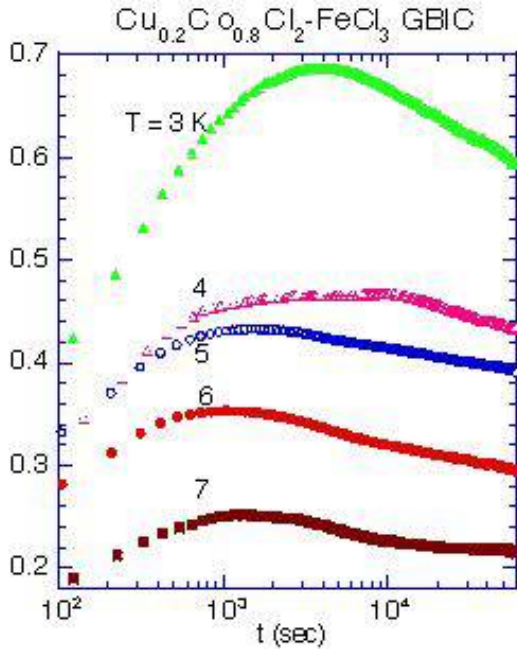


FIG. 15: t dependence of $S(t) \equiv (1/H) dM_{ZFC} / d \ln t$ at various T . $t_w = 2.0 \times 10^3$ sec.

TABLE II: Exponents b^0 and b^0 determined from the least squares fits of $\chi^0(t; f)$ and $\chi^0(t; f)$ at f to the power law form by given by Eq.(7) for $\chi^0(t; f)$ and the corresponding equation for $\chi^0(t; f)$. $T = 7$ and 8.5 K.

T (K)	f (Hz)	b^0	b^0	b^0	b^0
7	0.05	0.074	0.016	-	-
7	0.1	0.045	0.013	0.012	0.005
7	0.5	0.042	0.008	0.045	0.005
7	1	0.029	0.006	0.046	0.006
7	5	0.015	0.025	0.070	0.016
8.5	0.05	0.147	0.067	-	-
8.5	0.5	0.065	0.028	-	-
8.5	1	0.046	0.022	0.038	0.011

and T_c , while the value of a in $(Fe_{0.65}Ni_{0.35})_{0.882}Mn_{0.118}$ decreases with increasing T . We note that the T dependence of a in our system near T_c is similar to that in $Fe_{0.5}Mn_{0.5}TiO_3$ near T_{SG} ,³⁶ in spite of the fact that $Fe_{0.5}Mn_{0.5}TiO_3$ is a pure spin glass and undergoes a transition between the SG phase and the PM phase at T_{SG} . The values of M_{FC} and M_{ZFC} measured at $H = 10$ Oe (see Fig. 9(b)) are also listed in Table I. The value of M_1^0 is on the same order as that of M_{FC} and much larger than that of M_{ZFC} , where M_{FC} is close to thermodynamic equilibrium value. The prefactor M_2^0 decreases with increasing T and tends to reduce to zero around T_c .

We have measured the t dependence of χ^0 at $T = 7$ and 8.5 K, where $H = 0$. The system was quenched from 100 K to T at time (age) zero. Both χ^0 and χ^0 were measured simultaneously as a function of time t at constant T .

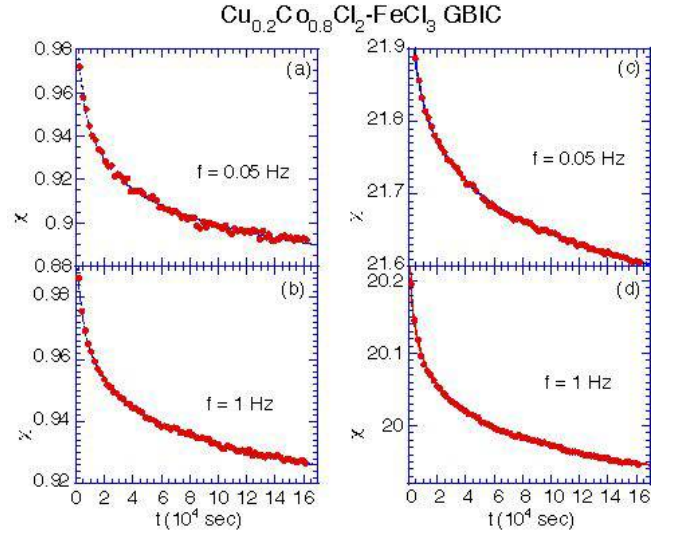


FIG. 16: t dependence of (a) and (b) χ^0 , and (c) and (d) χ^0 at $T = 7$ K for $f = 0.05$ and 1 Hz, where t is the time taken after the sample was quenched from 100 K to $T = 7$ K. $H = 0$. The solid lines denote the least squares fitting curves (see the text for detail).

Each point consists in the successive measurements at various frequencies ($0.05 \leq f \leq 1$ Hz). Figure 16 shows the t dependence of χ^0 and χ^0 at $T = 7$ K for $f = 0.05$ and 1 Hz, respectively. The absorption χ^0 decreases with increasing t and is well described by a power-law decay

$$\chi^0(t; f) = \chi_0^0(f) + A_0^0(f) t^{b^0}; \quad (7)$$

where b^0 is an exponent, and $\chi_0^0(f)$ and $A_0^0(f)$ are t -independent constants. In the limit of $t \rightarrow 1$, $\chi^0(t; f)$ tends to $\chi_0^0(f)$. The least squares fit of the data of $\chi^0(t; f)$ at $T = 7$ K to Eq.(7) yields parameters listed in Table II. The exponent b^0 , which is dependent on f , is smaller than that of the FM phase of reentrant ferromagnet $CdCr_{1.8}In_{0.2}S_4$ ($b^0 = 0.2$)¹² and the SG phase of pure spin glass $Fe_{0.5}Mn_{0.5}TiO_3$ ($b^0 = 0.14 - 0.03$).³⁷ The value of χ_0^0 tends to decrease with increasing f . In contrast, the value of A_0^0 tends to increase with increasing f . It follows that the second term of Eq.(7) cannot be described by a power form $(!t)^{b^0}$, suggesting no $!t$ -scaling law in the form of $\chi^0(!t)^{b^0}$. This is in contrast to the $!t$ -scaling of χ^0 in the FM phase of reentrant ferromagnet $CdCr_{1.8}In_{0.2}S_4$.¹² The t dependence of χ^0 can be also described by the power law form $(!t)^{b^0}$ which is similar to Eq.(7). The value of b^0 at $T = 7$ and 8.5 K which is listed in Table II, is on the same order as that of b^0 . Note that similar aging behavior is also observed both in χ^0 and χ^0 below T_{RSG} . The change of χ^0 and χ^0 with t below T_{RSG} is not so prominent compared to that above T_{RSG} , partly because of relatively small magnitude of χ^0 and χ^0 below T_{RSG} .

IV. DISCUSSION

The RSG phase below T_{RSG} is not a mixed phase but a normal SG phase. The static and dynamic behaviors of the RSG phase are characterized by that of the normal SG phase: a critical exponent $\beta = 0.57 \pm 0.10$, a dynamic critical exponent $x = 8.5 \pm 1.8$, and an exponent $p (= 1.55 \pm 0.13)$ for the AT line.³⁴ The aging phenomena are observed. The relaxation of $M_{ZFC}(t)$ obeys a stretched exponential law, which is usually used in analysis of the dynamics of the normal SG phase. No appreciable non-linear magnetic susceptibility is observed below T_{RSG} . These results suggest that the long-range ferromagnetic correlation completely disappears in the RSG phase.

In contrast, the FM phase of our system is very different from that of regular FM phase. The chaotic behavior observed in the FM phase is rather similar to that in the RSG phase. The prominent nonlinear susceptibility of the FM phase arises mainly from the unfrustrated ferromagnetically ordered spins (the FM network). The aging phenomena are also observed in the FM phase. A dynamic crossover of the relaxation of $M_{ZFC}(t)$ is observed around T_{RSG} . Above T_{RSG} the relaxation of $M_{ZFC}(t)$ obeys a weak power law. These results can be well explained in terms of the phenomenological random-eld picture proposed by Aeppli et al.⁶ (see Sec. I). The FM phase consists of the FM network (with slow dynamics) surrounded by frustrated spins (the PM clusters with fast dynamics). Such a nonuniformity gives rise to the chaotic nature of the FM phase. On approaching T_{RSG} from the high-T side, the thermal fluctuations of the spins in the PM clusters become so slow that the slow dynamics of the FM network is significantly influenced by the dynamics of the PM clusters. The coupling between the FM network and the PM clusters becomes important. The molecular fields from the slow PM spins act as a random magnetic field. This causes breakups of the FM network into finite-sized clusters. Below T_{RSG} , the system becomes into the RSG phase.

Next we discuss the nature of the aging phenomena in the FM phase. The features of the aging phenomena are summarized as follows. (i) $M_{ZFC}(t)$ has a power law form ($M_{ZFC} \propto t^{-a}$) for $5 \leq T \leq 9$ K. The value of a is listed in Table I. (ii) Both $\chi''(t;!)$ and $\chi''(t;!)^a$ at $T = 7$ and 8.5 K have power law forms ($\chi'' \propto t^{-b^0}$ and $\chi''^a \propto t^{-b^0}$) at fixed $f (= 1/2)$. The values of b^0 and b^0 are listed in Table II. (iii) $\chi''(!)$ for $6.1 \leq T \leq 7.3$ K has a power law form ($\chi'' \propto !^{-\omega}$), where $\omega = 0.04 \pm 0.01$ at 6.1 K and 0.12 ± 0.01 at 7.2 K. The increase of $\chi''(!)$ with increasing $!$ is similar to that reported in conventional SG's such as $Fe_{0.5}Mn_{0.5}TiO_3$.²⁶

As is listed in Table I, the exponent $a(T)$ increases exponentially with increasing T and is described by $a(T) = 0.23 \exp[(1/T - 1/T_c) \times 0.148]$ with $T_c = 9.7$ K. Similar result on $a(T)$ has been reported by Ito et al.³⁶ for the SG phase of $Fe_{0.5}Mn_{0.5}TiO_3$: $a(T) = 1.6 \exp[-(1/T - 1/T_{SG}(H))] \times 0.17g$ with $T_{SG}(H) = 17.6$ K at $H = 3.2$

kOe. From Monte-Carlo simulations on the 3D J Ising spin glass model, Ogilski²⁷ has discussed the temperature dependence of the order parameter $q(t)$ below the spin freezing temperature T_{SG} . The order parameter $q(t)$ is described by a power law form $q(t) \propto t^{-a(T)}$, where $a(T)$ is well fitted by $a(T) = 0.07 \exp[(1/T - 1/T_{SG}) \times 0.28]$; $a = 0.07$ at $T = T_{SG}$. The similarity between our result and the computer simulation is remarkable. This implies that the growth of M_{ZFC} in the FM phase (but not in the RSG phase) is essentially the same as that in the SG phase of spin glass systems.

What is the relation between the exponent a for $M_{ZFC}(t)$ and the exponent (b^0, b^0, ω) for χ'' and χ''^a ? According to Lundgren et al.,^{38,39} $M_{ZFC}(t)$ is related to the linear AC susceptibility $\chi''(!)$ and $\chi''(!)^a$ through the following relations

$$(1/H) dM_{ZFC} = d \ln t = 2^{-\omega}(!)^{-\omega}; \quad (t = 1/!); \quad (8)$$

and

$$1 - q(t) = (1/H) M_{ZFC}(t) = (!)^{-a}; \quad (t = 1/!); \quad (9)$$

When $M_{ZFC}(t)$ is described by a power law form given by Eq.(6), $\chi''(!)$ and $\chi''(!)^a$ can be estimated as $\chi''(!)^a \propto (!)^{-a}$ (or t^a) and $\chi''(!)^a \propto (!)^{-a}$ (or t^a), respectively, leading to a prediction that the exponents ω, b^0 , and b^0 are essentially the same as the exponent a . Experimentally we find $a = 0.059 \pm 0.001$ ($T = 8$ K), $b^0 = 0.074 \pm 0.016$ ($T = 7$ K and $f = 0.05$ Hz), and $b^0 = 0.046 \pm 0.006$ ($T = 7$ K, $f = 1$ Hz), and $\omega = 0.081 \pm 0.02$ ($T = 6.7$ K). There are relatively large differences among ω, b^0, b^0 , and a , depending on the conditions. Nevertheless, we can say that these exponents are roughly the same and are on the order of $0.05 - 0.08$ around 7 K. The value of these exponents is nearly equal to that of the exponent $y (= 0.066 \pm 0.001)$ derived from the scaling analysis in Sec. IIIB. Note that our result of a is in good agreement with $a = 0.060 - 0.088$ for the FM phase of the reentrant ferromagnet $(Fe_{0.65}Ni_{0.35})_{0.882}Mn_{0.118}$.³⁵

Finally we estimate the value of y . The exponent y is given by $y = -x$, where $x = z$. When we use the scaling relation, $\chi'' = 2^{-z}$, which is derived in our previous paper,²³ y is given by $y = 2^{-z}$, where z is the energy exponent and z is the dynamic critical exponent. The values of χ'' and z are theoretically predicted: $z = 6.0 \pm 0.5$ for the 3D J Ising spin glass model (Ogilski²⁷) and $z = 0.19 \pm 0.01$ (Bray and Moore⁴⁰). Using these values, y is estimated as $y = 0.063 \pm 0.017$, which is in good agreement with our result ($y = 0.066 \pm 0.001$).

V. CONCLUSION

The nonlinear susceptibility and aging phenomena are observed in the FM phase of the reentrant ferromagnet $Cu_{0.2}Co_{0.8}C_{12}FeCl_3$ GBIC. These results indicate that the FM phase between T_{RSG} and T_c has a chaotic nature. The absorption $\chi''(t;!)$ is described by a power law

form t^{b^0} but not by a t -scaling form $(t)^{b^0}$. A dynamic crossover behavior is observed around T_{RSG} . The time dependence of M_{ZFC} has a stretched-exponential form for the RSG phase, and a power-law form for the FM phase. Further studies on aging behaviors including memory effect, rejuvenation, and waiting time dependence, are required to understand the nature of the FM phase, with the same qualitative features as in conventional spin glasses.

Acknowledgments

We would like to thank H. Suematsu for providing us with single crystalline graphite, T.-Y. Huang for his assistance in susceptibility measurements, T. Shima and B. Olson for their assistance in sample preparation and x-ray characterization. Early work, in particular for the sample preparation, was supported by NSF DMR 9201656.

suzuki@binghamton.edu

itsuko@binghamton.edu

- ¹ K. Motoya, S. M. Shapiro, and Y. Muraoka, Phys. Rev. B 28, 6183 (1983).
- ² J. Suzuki, Y. Endoh, M. Arai, M. Furusaka, and H. Yoshizawa, J. Phys. Soc. Jpn. 59, 718 (1990).
- ³ J. A. Gehrig and S. M. Bhagat, J. Magn. Magn. Mater. 25, 17 (1981).
- ⁴ K. Jonason, J. Mattsson, and P. Nordblad, Phys. Rev. B 53, 6507 (1996).
- ⁵ K. Jonason, J. Mattsson, and P. Nordblad, Phys. Rev. Lett. 77, 2562 (1996).
- ⁶ G. Aeppli, S. M. Shapiro, R. J. Birgeneau, and H. S. Chen, Phys. Rev. B 28, 5160 (1983).
- ⁷ T. Sato, T. Ando, T. Ogawa, S. Morimoto, and A. Ito, Phys. Rev. B 64, 184432 (2001).
- ⁸ T. Ogawa, H. Nagasaki, and T. Sato, Phys. Rev. B 65, 024430 (2001).
- ⁹ J. L. Dormann, A. Sai, V. Cagan, and M. Nogues, Phys. Stat. Sol. (b) 131, 573 (1985).
- ¹⁰ M. Alba and J. Hammann, J. Magn. Magn. Mater. 54-57, 213 (1986).
- ¹¹ S. Pouget and M. Alba, J. Phys. Condens. Matter 7, 4739 (1995).
- ¹² V. Dupuis, E. Vincent, M. Alba, and J. Hammann, Eur. Phys. J. B 29, 19 (2002).
- ¹³ H. M. Aletta, G. Aeppli, and S. M. Shapiro, Phys. Rev. Lett. 48, 1490 (1982).
- ¹⁴ G. Aeppli, H. M. Aletta, S. M. Shapiro, and D. Abemathy, Phys. Rev. B 36, 3956 (1987).
- ¹⁵ P. Mathieu, P. Nordblad, D. N. H. Nam, N. X. Phuc, and N. V. Khien, Phys. Rev. B 63, 174405 (2001).
- ¹⁶ D. Sherrington and S. Kirkpatrick, Phys. Rev. Lett. 32, 1792 (1975).
- ¹⁷ S. F. Edwards and P. W. Anderson, J. Phys. F 5, 965 (1975).
- ¹⁸ G. Parisi, Phys. Rev. Lett. 43, 1754 (1979).
- ¹⁹ G. Toulouse, J. Phys. (France) Lett. 41, L447 (1980).
- ²⁰ I. S. Suzuki, M. Suzuki, H. Satoh, and T. Enoki, Solid State Commun. 104, 581 (1997).

- ²¹ I. S. Suzuki, M. Suzuki, H. Satoh, and T. Enoki, Mol. Cryst. and Liq. Cryst. 340, 107 (2000).
- ²² M. Suzuki and I. S. Suzuki, Phys. Rev. B 59, 4221 (1999).
- ²³ I. S. Suzuki and M. Suzuki, Phys. Rev. B (2003), in press.
- ²⁴ M. Suzuki, I. S. Suzuki, and T.-Y. Huang, J. Phys. Condensed Matter 14, 5583 (2002).
- ²⁵ T. Sato and Y. Miyako, J. Phys. Soc. Jpn. 51, 1394 (1981).
- ²⁶ K. Gunnarsson, P. Svedlindh, P. Nordblad, L. Lundgren, H. A. ruga, and A. Ito, Phys. Rev. Lett. 61, 754 (1988).
- ²⁷ A. T. Ogielski, Phys. Rev. B 32, 7384 (1985).
- ²⁸ W. Klemann, P. Petravic, Ch. Binek, G. N. Kakazei, Yu. G. Pogorelov, J. B. Sousa, C. Cardoso, and P. P. Freitas, Phys. Rev. B 63, 134423 (2001).
- ²⁹ S. Geschwind, D. A. Huse, and G. E. Devlin, Phys. Rev. B 41, 4854 (1990).
- ³⁰ K. Gunnarsson, P. Svedlindh, P. Nordblad, L. Lundgren, H. A. ruga, and A. Ito, Phys. Rev. B 43, 8199 (1991).
- ³¹ W. Klemann, J. S. Kouvel, and H. Claus, Phys. Rev. B 30, 6480 (1984).
- ³² W. Klemann and J. S. Kouvel, Phys. Rev. B 35, 1764 (1987).
- ³³ B. K. Srivastava, A. Krishnamurthy, V. Ghose, J. Mattsson, and P. Nordblad, J. Magn. Magn. Mater. 132, 124 (1994).
- ³⁴ J. R. L. de Almeida and D. J. Thouless, J. Phys. A 11, 983 (1978).
- ³⁵ D. Li, R. M. Roshko, and G. Yang, Phys. Rev. B 49, 9601 (1994).
- ³⁶ A. Ito, H. A. ruga, E. Torikai, M. Kikuchi, Y. Syono, and H. Takei, Phys. Rev. Lett. 57, 483 (1986).
- ³⁷ V. Dupuis, E. Vincent, J.-P. Bouchaud, J. Hammann, A. Ito, and H. A. ruga Katori, Phys. Rev. B 64, 174204 (2001).
- ³⁸ L. Lundgren, in Relaxation in Complex Systems and Related Topics, edited by I. A. Campbell and C. Giovannella (Plenum Press, New York, 1990) p.3.
- ³⁹ L. Lundgren, P. Svedlindh, and O. Beckman, Phys. Rev. B 26, 3990 (1982).
- ⁴⁰ A. J. Bray and M. A. Moore, Phys. Rev. Lett. 58, 57 (1987).